Journal of Computational and Applied Mathematics 235 (2011) 1885–1896

Contents lists available at ScienceDirect

Journal of Computational and Applied Mathematics

journal homepage: www.elsevier.com/locate/cam

Minimum-energy wavelet frame on the interval with arbitrary integer dilation factor☆

Cao Chunhong, Gao Xieping*

College of Information and Engineering, Xiangtan University, Xiangtan, 411105, China

ARTICLE INFO

Article history:
Received 5 July 2008
Received in revised form 10 February 2010

Keywords:
Scaling function
Multi-resolution analysis
Frame
Minimum-energy

ABSTRACT

In this paper, we study minimum-energy frame $\Psi = \{\psi^1, \psi^2, \ldots, \psi^M\}$ on the interval with arbitrary factor d for $L^2[0, 1]$, Ψ corresponding to some refinable functions with compact support. We give the constructive proof as well as the necessary and sufficient conditions of minimum-energy frames for $L^2[0, 1]$, present the decomposition and reconstruction formulas of minimum-energy frame on the interval [0, 1], and some examples. The experimental results show that the proposed minimum-energy frame on the interval improves the performance in the application of image denoising significantly.

Contents

1. Introduction

This paper is concerned with the study of compactly supported tight frames as a replacement of compactly supported orthonormal wavelets when the system $\{\phi(\cdot - k) : k \in Z\}$ generated by the corresponding compactly supported scaling function ϕ is not orthogonal and, more generally, when ϕ is simply a refinable function (meaning that $\{\phi(\cdot - k) : k \in Z\}$ may not be stable).

Both orthogonal and biorthogonal wavelets on the real line have been proved to be very useful in various applications. However, in many applications, one is interested in problems confined to an interval such as solutions to differential equations with boundary conditions and image processing. An excellent construction of orthogonal wavelet based on the interval was given in [1] by adapting the famous Daubechies orthogonal wavelets on the real line to the interval. With

☆ Supported by the Natural Science Foundation of China (Grant No. 60375021).
* Corresponding author.
E-mail address: xpgao@xtu.edu.cn (X. Gao).

0377-0427/$ – see front matter © 2010 Elsevier B.V. All rights reserved.
doi:10.1016/j.cam.2010.12.009

the exception of the first order cardinal B-spline and its corresponding Haar function, however, any compactly supported orthonormal scaling function and its corresponding MRA (Multi-Resolution Analysis) wavelet do not have the symmetry or anti-symmetry property. For this and other reasons, biorthogonal scaling functions and wavelets with compact support were introduced by Cohen et al. by using two different MRAs. One of the disadvantages of this biorthogonal approach is that since two different MRAs are used, the analysis and synthesis operations of biorthogonal wavelet pair $(\psi, \widetilde{\psi})$ cannot be interchanged at any particular scale d^{j_0}. In other words, 'change-of-bases' between $\{\psi_{j_0,k} : k \in Z\}$ and $\{\widetilde{\psi}_{j_0,k} : k \in Z\}$ is not possible [2].

Fortunately, besides orthonormal wavelets, minimum-energy frames can well avoid the complication of change of bases but still use the same wavelets both for analysis and synthesis. Recently, wavelet tight frames have been attracted more and more attention, just because they have good time-frequency location property, shift-invariance, and more design freedom. In addition, for their stability in signal reconstruction, wavelet tight frames have been widely applied in signal processing.

Wavelet frames have received increased attention in the literature [3–15], however, interval wavelet frame has not yet been concerned. The main purpose of this paper is to study minimum-energy frame on the interval with arbitrary factor d. Firstly, we construct a class of minimum-energy wavelet frames with arbitrary factor d for $L^2[0, 1]$, which not only allow the design more freedom, can have the properties in the applications with symmetry and/or anti-symmetry, compact supports, good time-frequency localized property and shift-invariance, but also can solve the un-matching problem between the space of $L^2(R)$ and the signal space of $L^2(K)$ (K denotes a finite region). And then we obtain the necessary and sufficient conditions of minimum-energy wavelet frames for $L^2[0, 1]$. Moreover, we give the decomposition and reconstruction algorithms, and some examples of minimum-energy wavelet frames for $L^2[0, 1]$. In the final, we apply minimum-energy frame on the interval to image denoising. The experimental results show that the proposed algorithm improves the denoising performance significantly.

2. Preliminaries

In this paper, K is the set of integers, R is the set of real numbers, d is integer number and $d \geq 2$. We shall consider only functions of one variable in the space $L^2(R)$ with the inner product $\langle f, g\rangle = \int_{-\infty}^{+\infty} f(x)\overline{g(x)}\mathrm{d}x$, the Fourier transform $\hat{f}(\omega) = \int_{-\infty}^{+\infty} f(x)e^{-i\omega x}\mathrm{d}x$.

Definition 1. Let H be a Hilbert space, $\{h_k\}_{k\in Z} \subset H$, if there exist constants $A > 0, B < \infty$, such that for any $f \in H$, there is $A\|f\|^2 \leq \sum_{k\in Z} |\langle f, h_k\rangle|^2 \leq B\|f\|^2$, then $\{h_k\}_{k\in Z}$ is a frame, B, A is up and below frame bounds of the frame; if $A = B$, the frame is called tight frame; if $A = B = 1$, is called normal tight frame.

Definition 2. For wavelet function $\psi(x)$ for $L^2(R)$, $a > 1, b > 0$, if $\{\psi_{j,k}(x) = a^{j/2}\psi(a^j x - kb), j, k \in Z\}$ span a frame for $L^2(R)$, then the frame is called affine (or wavelet) frame, and (ψ, a, b) is called the generators of the frame.

Definition 3. Assume $\phi \in L^2(R)$, $V_j = span\{d^{j/2}\phi(d^j \cdot -k), k \in Z\}, j \in Z$, if the subspace V_j satisfy:

(1) $V_j \subset V_{j+1}, \forall j \in Z$;
(2) $\bigcup_{j\in Z} V_j = L^2(R), \bigcap_{j\in Z} V_j = \{0\}$;
(3) $f(\cdot) \in V_j$ if and only if $f(d\cdot) \in V_{j+1}, \forall j \in Z$
(4) $f(\cdot) \in V_j$ if and only if $f(\cdot + \frac{1}{d^j}) \in V_j, \forall j \in Z$
(5) $\{\phi(\cdot - k), k \in Z\}$ is a frame of space V_0;

then ϕ is called scaling function, and we say that ϕ generates a *FMRA*(V_j) (Frame Multi-Resolution Analysis) for $L^2(R)$, abbreviated as *FMRA*.

Definition 4. Assume $\Psi = \{\psi^1, \psi^2, \ldots, \psi^M\} \subset L^2(R)$, V_j is spanned by scaling function in sense of Definition 3, if $\Psi \subset V_1$ and satisfies: $\sum_{i=1}^{M}\sum_{j,k\in Z} |\langle f, \psi^i_{j,k}\rangle|^2 = \|f\|^2$, where $\psi^i_{j,k} = d^{j/2}\psi^i(d^j \cdot -k)$, we say $\Psi = \{\psi^1, \psi^2, \ldots, \psi^M\} \subset L^2(R)$ is a *MRA* frame generated by scaling function ϕ.

Definition 5. Let $\phi \in L^2(R)$, with $\hat{\phi} \in L^\infty$, $\hat{\phi}$ continuous at 0, and $\hat{\phi}(0) = 1$, be a refinable function that generates the nested subspaces $\{V_j\}_{j\in Z}$, then $\Psi = \{\psi^1, \psi^2, \ldots, \psi^M\} \subset V_1$ is called a minimum-energy (wavelet) frame associated with ϕ, if

$$\sum_{k\in Z} |\langle f, \phi_{1,k}\rangle|^2 = \sum_{k\in Z} |\langle f, \phi_{0,k}\rangle|^2 + \sum_{i=1}^{M}\sum_{k\in Z} |\langle f, \psi^i_{0,k}\rangle|^2 \tag{1}$$

where $\phi_{j,k} = d^{j/2}\phi(d^j \cdot -k)$.

Remark 1. By the parseval identity, a minimum-energy frame ψ is necessarily a tight frame for $L^2(R)$, with frame bound equal to 1.

Remark 2. The formulation (1) is equivalent to the formulation

$$\sum_{k\in Z}\langle f, \phi_{1,k}\rangle\phi_{1,k} = \sum_{k\in Z}\langle f, \phi_{0,k}\rangle\phi_{0,k} + \sum_{i=1}^{M}\sum_{k\in Z}\langle f, \psi^i_{0,k}\rangle\psi^i_{0,k}. \tag{2}$$

3. Main results

3.1. The notion of FMRA on the interval [0, 1]

Let $\gamma = 2N$ or $\gamma = 2N+1$, N be a positive integer number, K' be a positive number, $j_0 = min\{j : d^j \geq \gamma\}$, $N' = (d-1)\gamma - dN$.

Definition 6. Frame multi-Resolution Analysis on the interval [0, 1] is the nested subspaces $V_j \subset L^2[0,1]$, which satisfy:

(1) $V_j \subset V_{j+1}, j \geq j_0$;
(2) $\bigcup_{j\geq j_0} V_j = L^2[0,1]$, $\bigcap_{j\geq j_0} V_j = \{0\}$;
(3) $f(\cdot) \in V_j$ if and only if $f(d\cdot) \in V_{j+1}, j \geq j_0$;
(4) $f(\cdot) \in V_j$ if and only if $f(\cdot + \frac{1}{d^j}) \in V_j, j \geq j_0$;
(5) Family of $\{\phi(\cdot - k), 0 \leq k \leq K'\}$, $supp(\phi) = [0, \gamma]$, is a frame of space V_0;

then ϕ is called scaling function, and we say ϕ generates a *FMRA*(V_j) for $L^2[0,1]$, abbreviated as *FMRA*($V_j[0,1]$).

Let $V_{j+1}[0,1] := V_j[0,1] + U_j[0,1]$, but this is not a direct sum decomposition, because $V_j[0,1] \bigcap U_j[0,1] \neq 0$. If there exist functions $\psi^1, \psi^2, \ldots, \psi^M$ such that for any $j \geq j_0$, the family $\{\psi^i(\cdot - k), 0 \leq k \leq K, i = 1, \ldots, M\}$ is a frame of space U_0, then we say $\psi^1, \psi^2, \ldots, \psi^M$ is a wavelet frame for $L^2[0,1]$.

3.2. Characterization of minimum-energy FMRA on the interval [0, 1]

In this section, we give a complete characterization of minimum-energy frames associated with some given refinable function in term of their two-scale symbols. For convenience, we only consider symbols in the Winner class $\mathcal{W}$, meaning that the coefficient sequences of the symbols are in l^1. Let $\phi \in L^2$, with $\hat{\phi} \in L^2$, $\hat{\phi}$ continuous at 0, and $\hat{\phi}(0) = 1$, be a refinable function with refinement equation $\phi(x) = \sum_{k\in Z} p_k\phi(dx - k)$ such that its two-scale symbol $P(z) = \frac{1}{d}\sum_{k\in Z} p_k z^k$ is in $\mathcal{W}$. Consider $\Psi = \{\psi^1, \psi^2, \ldots, \psi^M\} \subset V_1$, with $\psi^i(x) = \sum_{k\in Z} q^i_k\phi(dx - k)$, $i = 1, \ldots, M$, and two-scale symbol $Q^i(z) = \frac{1}{d}\sum_{k\in Z} q^i_k z^k$, $i = 1, \ldots, M$.

Theorem 1. *Define left scaling function $\phi^L_{j,k}(x)$ and right scaling function $\phi^R_{j,k}(x)$ as follows*

$$\phi^L_{j,k}(x) = \sum_{n=\gamma+1}^{k-N} C_{k,n}\phi_{j,n}(x)|_{[0,1]}, \quad 0 \leq k \leq N-1$$

$$\phi^R_{j,k}(x) = \sum_{n=d^j-\gamma+N-k}^{d^j-1} C'_{k,n}\phi_{j,n}(x)|_{[0,1]}, \quad 0 \leq k \leq N-1$$

let $\Phi_j = \{\phi^L_{j,k}, k = 0, \ldots, N-1, \phi_{j,k}, k = 0, \ldots, d^j - \gamma, \phi^R_{j,k}, k = 0, \ldots, N-1\}$, if $C_{k,n}$, $C'_{k,n}$ are constants such that $\{\phi^L_{j,k}, k = 0, \ldots, N-1\}$, $\{\phi^R_{j,k}, k = 0, \ldots, N-1\}$ satisfy frame condition, then there exist constants $H^L_{k,n}$, $H^R_{k,n}$, $h^L_{k,n}$, $h^R_{k,n}$, such that Φ_j satisfies two-scale equations

$$\sqrt{d}\phi^L_{j,k} = \sum_{n=0}^{N-1} H^L_{k,n}\phi^L_{j+1,n} + \sum_{n=0}^{dk+N'} h^L_{k,n}\phi_{j+1,n}, \quad 0 \leq k \leq N-1 \tag{3}$$

$$\sqrt{d}\phi_{j,k} = \sum_{n=dk}^{dk+\gamma} H_{n-dk}\phi_{j+1,n}, \quad 0 \leq k \leq d^j - \gamma \tag{4}$$

$$\sqrt{d}\phi^R_{j,k} = \sum_{n=0}^{dk+N'} h^R_{k,n}\phi_{j+1,d^{j+1}-\gamma-n} + \sum_{n=0}^{N-1} H^R_{k,n}\phi^R_{j+1,n}, \quad 0 \leq k \leq N-1 \tag{5}$$

and for any $j \geq \lceil \log_d \gamma \rceil$, ϕ_j is a frame for $V_j[0,1]$. Where $\lceil x \rceil$ denotes the smallest integer not less than x.

Proof. We give the proof of Φ_j is a frame for $V_j[0,1]$.

For $\{\phi^L_{j,k}, k=0,\dots,N-1\}$ and $\{\phi^R_{j,k}, k=0,\dots,N-1\}$ satisfy frame condition respectively, i.e., there exist constants $0 \le A_1 \le B_1 < \infty$, $0 \le A_2 \le B_2 < \infty$ such that for any $f \in L^2(R)$, $A_1\|f\|^2 \le \sum_{j\ge j_0,0\le k\le N-1} |\langle f, \phi^L_{j,k}\rangle|^2 \le B_1\|f\|^2$, $A_2\|f\|^2 \le \sum_{j\ge j_0,0\le k\le N-1} |\langle f, \phi^R_{j,k}\rangle|^2 \le B_2\|f\|^2$. And ϕ is a frame scaling function for $L^2(R)$, then $\{\phi_{j,k}, k=0,\dots,d^j-\gamma\}$ satisfies frame condition, i.e., there exist constants $0 \le A_3 \le B_3 < \infty$ such that for any $f \in L^2(R)$, $A_3\|f\|^2 \le \sum_{j\ge j_0,0\le k\le d^j-\gamma} |\langle f, \phi_{j,k}\rangle|^2 \le B_3\|f\|^2$, then there exist constants $A = A_1+A_2+A_3$, $B = B_1+B_2+B_3$, $0 \le A \le B < \infty$, such that for any $f \in L^2(R)$, $A\|f\|^2 \le \sum_{j\ge j_0} |\langle f, \phi_{j,k}\rangle_{[0,1]}|^2 \le B\|f\|^2$. One obtains that Φ_j is a frame for $V_j[0,1]$.

The deduction of two-scale equations is similar to the deduction of Theorem 1 in the paper [16]. □

Theorem 2. *Assume that $\psi^{L,i}_{j,k}, k=0,\dots,N-1$, $\psi^i_{j,k}, k=0,\dots,d^j-\gamma$, $\psi^{R,i}_{j,k}, k=0,\dots,N-1, i=1,\dots,M$, are expressed as follows:*

$$\sqrt{d}\psi^{L,i}_{j,k} = \sum_{n=0}^{N-1} G^{L,i}_{k,n}\phi^L_{j+1,n} + \sum_{n=0}^{dk+N'} g^{L,i}_{k,n}\phi_{j+1,n}, \quad 0 \le k \le N-1, i=1,\dots,M \tag{6}$$

$$\sqrt{d}\psi^i_{j,k} = \sum_{n=dk}^{dk+\gamma} G^i_{n-dk}\phi_{j+1,n}, \quad 0 \le k \le d^j-\gamma, i=1,\dots,M \tag{7}$$

$$\sqrt{d}\psi^{R,i}_{j,k} = \sum_{n=0}^{dk+N'} g^{R,i}_{k,n}\phi_{j+1,d^{j+1}-\gamma-n} + \sum_{n=0}^{N-1} G^{R,i}_{k,n}\phi^R_{j+1,n}, \quad 0 \le k \le N-1, i=1,\dots,M \tag{8}$$

let $\Psi_j = \{\psi^{L,i}_{j,k}, k=0,\dots,N-1, \psi^i_{j,k}, k=0,\dots,d^j-\gamma, \psi^{R,i}_{j,k}, k=0,\dots,N-1, i=1,\dots,M\}$, if $\{G^{L,i}_{k,n}\}$, $\{g^{L,i}_{k,n}\}$, $\{G^{R,i}_{k,n}\}$, $\{g^{R,i}_{k,n}\}$ are constants such that $\{\psi^{L,i}_{j,k}(x), k=0,\dots,N-1\}$ and $\{\psi^{R,i}_{j,k}(x), k=0,\dots,N-1\}$ satisfy frame condition, then for any $j \ge \lceil \log_d \gamma \rceil$, ψ_j is a frame for $U_j[0,1]$.

The proof is similar to Theorem 1.

For convenience, we denote

(1) $S_j = \{k | -N \le k \le d^j-\gamma+N\}$

$$H = \begin{pmatrix} H^{LL} & H^{LI} & 0 \\ 0 & H^{II} & 0 \\ 0 & H^{RI} & H^{RR} \end{pmatrix}, \qquad G^i = \begin{pmatrix} G^{LL}_i & G^{LI}_i & 0 \\ 0 & G^{II}_i & 0 \\ 0 & G^{RI}_i & G^{RR}_i \end{pmatrix}$$

$D_j = \mathrm{diag}(e^{i\omega(-N)/d^j}, e^{i\omega(-N+1)/d^j}, \dots, e^{i\omega(d^j-\gamma+N)/d^j})$, $P(z) = (1/d)D_j^{-1}HD_{j+1}$, $Q^i(z) = (1/d)D_j^{-1}G^iD_{j+1}$.

(2) The structured scaling functions in Theorem 1 are expressed as

$$\phi_{j,k} = \begin{cases} \phi^L_{j,N+k}, & k=-N,\dots,-1, \\ \phi_{j,k}, & k=0,\dots,d^j-\gamma, \\ \phi^R_{j,k-(d^j-\gamma)-1}, & k=d^j-\gamma+1,\dots,d^j-\gamma+N. \end{cases}$$

(3) The structured wavelet functions in Theorem 2 are expressed as

$$\psi^i_{j,k} = \begin{cases} \psi^{L,i}_{j,N+k}, & k=-N,\dots,-1, \\ \psi^i_{j,k}, & k=0,\dots,d^j-\gamma. \\ \psi^{R,i}_{j,k-(d^j-\gamma)-1}, & k=d^j-\gamma+1,\dots,d^j-\gamma+N. \end{cases}$$

Then $\hat\phi(\omega) = P(z)\hat\phi(\frac{\omega}{d})$, $\hat\psi^i(\omega) = Q^i(z)\hat\phi(\frac{\omega}{d})$, $i=1,\dots,M$.

Theorem 3. *Let $\psi^{L,i}_{j,k}, k=0,\dots,N-1$, $\psi^i_{j,k}, k=0,\dots,d^j-\gamma$, $\psi^{R,i}_{j,k}, k=0,\dots,N-1, i=1,\dots,M$, be defined as (6)–(8), then the following statements are equivalent:*

(1) *$\Psi_j = \{\psi^{L,i}_{j,k}, k=0,\dots,N-1, \psi^i_{j,k}, k=0,\dots,d^j-\gamma, \psi^{R,i}_{j,k}, k=0,\dots,N-1, i=1,\dots,M\}$ is a minimum-energy tight frame for $L^2[0,1]$.*

(2)

$$d\left(P^*(z)P(z) + \sum_{i=1}^{M}(Q^i(z))^*Q^i(z)\right) = I_{|S_{j+1}|}, \ |z|=1 \tag{9}$$

(3)

$$\sum_{k\in S_j}\left(H_{k,m}H_{k,l}+\sum_{i=1}^{M}G^i_{k,m}G^i_{k,l}\right)-d\delta_{m,l}=0,\quad \forall m,l\in S_{j+1} \tag{10}$$

where * represents the conjugate of the transpose, $\delta_{j,k}$ is the Kronecker symbol.

Proof. Let $\alpha_{m,l}:=\sum_{k\in S_j}(H_{k,m}H_{k,l}+\sum_{i=1}^{M}G^i_{k,m}G^i_{k,l})-d\delta_{m,l}$, by using two-scale relations (3)–(8), formula (2) can be written as

$$\begin{aligned}
&\sum_{k\in S_{j+1}}\langle f,\phi_{j+1,k}\rangle\phi_{j+1,k}=\sum_{k\in S_j}\langle f,\phi_{j,k}\rangle\phi_{j,k}+\sum_{i=1}^{M}\sum_{k\in S_j}\langle f,\psi^i_{j,k}\rangle\psi^i_{j,k}\\
&=\sum_{k\in S_j}\left\langle f,\frac{\sqrt{d}}{d}\sum_{l\in S_{j+1}}H_{k,l}\phi_{j+1,l}\right\rangle\frac{\sqrt{d}}{d}\sum_{l\in S_{j+1}}H_{k,l}\phi_{j+1,l}+\sum_{i=1}^{M}\sum_{k\in S_j}\left\langle f,\frac{\sqrt{d}}{d}\sum_{l\in S_{j+1}}G^i_{k,l}\phi_{j+1,l}\right\rangle\frac{\sqrt{d}}{d}\sum_{l\in S_{j+1}}G^i_{k,l}\phi_{j+1,l}\\
&=\frac{1}{d}\sum_{l\in S_{j+1}}\sum_{m\in S_{j+1}}\sum_{k\in S_j}\left(H_{k,m}H_{k,l}+\sum_{i=1}^{M}G^i_{k,m}G^i_{k,l}\right)\langle f,\phi_{j+1,m}\rangle\phi_{j+1,l}\\
&\Leftrightarrow\sum_{l\in S_{j+1}}\sum_{m\in S_{j+1}}\left\{\sum_{k\in S_j}\left(H_{k,m}H_{k,l}+\sum_{i=1}^{M}G^i_{k,m}G^i_{k,l}\right)-d\delta_{m,l}\right\}\langle f,\phi_{j+1,m}\rangle\phi_{j+1,l}=0\\
&\Leftrightarrow\sum_{l\in S_{j+1}}\sum_{m\in S_{j+1}}\alpha_{m,l}\langle f,\phi_{j+1,m}\rangle\phi_{j+1,l}=0,\quad f\in L^2.
\end{aligned} \tag{11}$$

We multiply the identities in (9) by the vector $(\hat\phi(\frac{\omega}{d})\dots\hat\phi(\frac{\omega}{d}))^T$ to obtain

$$\begin{aligned}
&2\left(P^*(z)\begin{pmatrix}\hat\phi(\omega)\\ \vdots\\ \hat\phi(\omega)\end{pmatrix}+\sum_{i=1}^{M}(Q^i(z))^*\begin{pmatrix}\hat\psi^1(\omega)\\ \vdots\\ \hat\psi^M(\omega)\end{pmatrix}\right)=\begin{pmatrix}\hat\phi\left(\frac{\omega}{d}\right)\\ \vdots\\ \hat\phi\left(\frac{\omega}{d}\right)\end{pmatrix}\\
&\Leftrightarrow d\left((D_j^{-1}HD_{j+1})^*\begin{pmatrix}\hat\phi(\omega)\\ \vdots\\ \hat\phi(\omega)\end{pmatrix}+\sum_{i=1}^{M}(D_j^{-1}G^iD_{j+1})^*\begin{pmatrix}\hat\psi^1(\omega)\\ \vdots\\ \hat\psi^M(\omega)\end{pmatrix}\right)=\begin{pmatrix}\hat\phi\left(\frac{\omega}{d}\right)\\ \vdots\\ \hat\phi\left(\frac{\omega}{d}\right)\end{pmatrix}\\
&\Leftrightarrow H^*\sqrt{d}\begin{pmatrix}\phi_{j,-N}\\ \vdots\\ \phi_{j,d^j-\gamma+N}\end{pmatrix}+\sum_{i=1}^{M}(G^i)^*\sqrt{d}\begin{pmatrix}\psi^1_{j,-N}\\ \vdots\\ \psi^M_{j,d^j-\gamma+N}\end{pmatrix}=d\begin{pmatrix}\phi_{j+1,-N}\\ \vdots\\ \phi_{j+1,d^{j+1}-\gamma+N}\end{pmatrix}\\
&\Leftrightarrow H^*H\begin{pmatrix}\phi_{j+1,-N}\\ \vdots\\ \phi_{j+1,d^{j+1}-\gamma+N}\end{pmatrix}+\sum_{i=1}^{M}(G^i)^*G^i\begin{pmatrix}\phi_{j+1,-N}\\ \vdots\\ \phi_{j+1,d^{j+1}-\gamma+N}\end{pmatrix}=d\begin{pmatrix}\phi_{j+1,-N}\\ \vdots\\ \phi_{j+1,d^{j+1}-\gamma+N}\end{pmatrix}\\
&\Leftrightarrow\left(H^*H+\sum_{i=1}^{M}(G^i)^*G^i\right)\begin{pmatrix}\phi_{j+1,-N}\\ \vdots\\ \phi_{j+1,d^{j+1}-\gamma+N}\end{pmatrix}=d\begin{pmatrix}\phi_{j+1,-N}\\ \vdots\\ \phi_{j+1,d^{j+1}-\gamma+N}\end{pmatrix}\\
&\Leftrightarrow\sum_{m\in S_{j+1}}\sum_{k\in S_j}H_{k,l}H_{k,m}\phi(d^{j+1}x-m)+\sum_{i=1}^{M}\sum_{k\in S_j}G^i_{k,l}\sum_{m\in S_{j+1}}G^i_{k,m}\phi(d^{j+1}x-m)=\phi(d^{j+1}x-l),\ l\in S_{j+1}\\
&\Leftrightarrow\sum_{m\in S_{j+1}}\alpha_{m,l}\phi_{j+1,m}=0,\ l\in S_{j+1}.
\end{aligned} \tag{12}$$

(13)

Hence, the proof of Theorem 3 reduces to the proof of the equivalence of (11), (13) and (10). It is obvious that (10) $\Rightarrow$ (13) $\Rightarrow$ (11). To show that (11) $\Rightarrow$ (10), let $f\in L^2$ be any compactly function, and $\beta_l(f):=\sum_{m\in S_{j+1}}\alpha_{m,l}\langle f,\phi_{j+1,m}\rangle$, $l\in S_j$, by taking the Fourier transform of formula (11), that the trigonometric $\sum_{l\in S_{j+1}}\beta_l(f)e^{-il\omega/d^{j+1}}=0$, so that $\beta_l(f)=0$, or

equivalently $\langle f, \sum_{m\in S_{j+1}} \alpha_{m,l}\phi_{j+1,m}\rangle = 0$. By choosing f to be a compactly supported function for $L^2(R)$, it follows that $\sum_{m\in S_{j+1}} \alpha_{m,l}\phi_{j+1,m} = 0$, Which implies that the trigonometric polynomial $\sum_{m\in S_{j+1}} \alpha_{m,l}e^{-il\omega/d^{j+1}}$ is identically equal to 0, so that $\alpha_{m,l} = 0$, $m, l \in S_{j+1}$. We complete the proof of Theorem 3. □

Theorem 4. *Minimum-energy tight frame for $L^2[0, 1]$ has decomposition and reconstruction algorithm as follows*
(1) *Decomposition algorithm*

$$\sqrt{d}c^L_{j,k} = \sum_{n=0}^{N-1} H^L_{k,n}c^L_{j+1,n} + \sum_{n=0}^{dk+N'} h^L_{k,n}c_{j+1,n}, \quad 0 \le k \le N-1,$$

$$\sqrt{d}c_{j,k} = \sum_{n=0}^{\gamma} H_n c_{j+1,n+dk}, \quad 0 \le k \le d^j - \gamma,$$

$$\sqrt{d}c^R_{j,k} = \sum_{n=0}^{dk+N'} h^R_{k,n}c_{j+1,d^{j+1}-\gamma-n} + \sum_{n=0}^{N-1} H^R_{k,n}c^R_{j+1,n}, \quad 0 \le k \le N-1,$$

$$\sqrt{d}d^{L,i}_{j,k} = \sum_{n=0}^{N-1} G^{L,i}_{k,n}c^L_{j+1,n} + \sum_{n=0}^{dk+N'} g^{L,i}_{k,n}c_{j+1,n}, \quad 0 \le k \le N-1,\ 1 \le i \le M,$$

$$\sqrt{d}d^i_{j,k} = \sum_{n=0}^{\gamma} G^i_n c_{j+1,n+dk}, \quad 0 \le k \le d^j - \gamma,\ 1 \le i \le M,$$

$$\sqrt{d}d^{R,i}_{j,k} = \sum_{n=0}^{dk+N'} g^{R,i}_{k,n}c_{j+1,d^{j+1}-\gamma-n} + \sum_{n=0}^{N-1} G^{R,i}_{k,n}c^R_{j+1,n}, \quad 0 \le k \le N-1,\ 1 \le i \le M.$$

(2) *Reconstruction algorithm*

$$\sqrt{d}c^L_{j+1,n} = \sum_{n=0}^{N-1} H^L_{k,n}c^L_{j,k} + \sum_{i=1}^{M}\sum_{n=0}^{N-1} G^{L,i}_{k,n}d^{L,i}_{j,k}, \quad 0 \le n \le N-1,$$

$$\sqrt{d}c^R_{j+1,n} = \sum_{n=0}^{N-1} H^R_{k,n}c^R_{j,k} + \sum_{i=1}^{M}\sum_{n=0}^{N-1} G^{R,i}_{k,n}d^{R,i}_{j,k}, \quad 0 \le n \le N-1,$$

$$\sqrt{d}c_{j+1,n} = \sum_{k=0}^{n} h^L_{k,n}c^L_{j,k} + \sum_{i=1}^{M}\sum_{k=0}^{n} g^{L,i}_{k,n}d^{L,i}_{j,k} + \sum_k H_{n-dk}c_{j,k} + \sum_{i=1}^{M}\sum_k G^i_{n-dk}d^i_{j,k}, \quad 0 \le n \le \gamma - 2,$$

$$\sqrt{d}c_{j+1,n} = \sum_k H_{n-dk}c_{j,k} + \sum_{i=1}^{M}\sum_k G^i_{n-dk}d^i_{j,k}, \quad \gamma - 1 \le n \le d^{j+1} - 2\gamma + 1,$$

$$\sqrt{d}c_{j+1,n} = \sum_{k=0}^{n} h^R_{k,n}c^R_{j,k} + \sum_{i=1}^{M}\sum_{k=0}^{n} g^{R,i}_{k,n}d^{R,i}_{j,k} + \sum_k H_{n-dk}c_{j,k} + \sum_{i=1}^{M}\sum_k G^i_{n-dk}d^i_{j,k},$$
$$d^{j+1} - 2\gamma + 2 \le n \le d^{j+1} - \gamma.$$

Proof. For $\forall f \in L^2$, let $c_{j,k} = \langle f, \phi_{j,k}\rangle$, $c^L_{j,k} = \langle f, \phi^L_{j,k}\rangle$, $c^R_{j,k} = \langle f, \phi^R_{j,k}\rangle$, $d^i_{j,k} = \langle f, \psi^i_{j,k}\rangle$, $d^{L,i}_{j,k} = \langle f, \psi^{L,i}_{j,k}\rangle$, $d^{R,i}_{j,k} = \langle f, \psi^{R,i}_{j,k}\rangle$, $i = 1, \ldots, M$. By using the two-scale relations (3)–(5) and (6)–(8), we obtain the decomposition algorithm, and taking the inner product of formula (12) with f, we obtain the reconstruction algorithm. □

4. Some examples

It is well known that the mth order cardinal B-spline $N_m(x)$ has the two-scale relation $\hat{N}_m(\omega) = P^d_m(z)N_m(\frac{\omega}{d})$, where $z = e^{-i\omega/d}$ and $P^d_m(z) = (\frac{1+z+\cdots+z^{d-1}}{d})^m$. By Theorem 2 in [2] and Theorem 3 in [3], there exists a minimum-energy frame $\{\psi^1_m, \psi^2_m, \ldots, \psi^M_m\}$.

4.1. $d = 2$

Example 1 (*Linear B-spline*). $P^2_2(z) = \frac{1}{4} + \frac{1}{2}z + \frac{1}{4}z^2, Q_1(z) = -\frac{1}{4} + \frac{1}{2}z - \frac{1}{4}z^2, Q_2(z) = \frac{\sqrt{2}}{4} - \frac{\sqrt{2}}{4}z^2$.

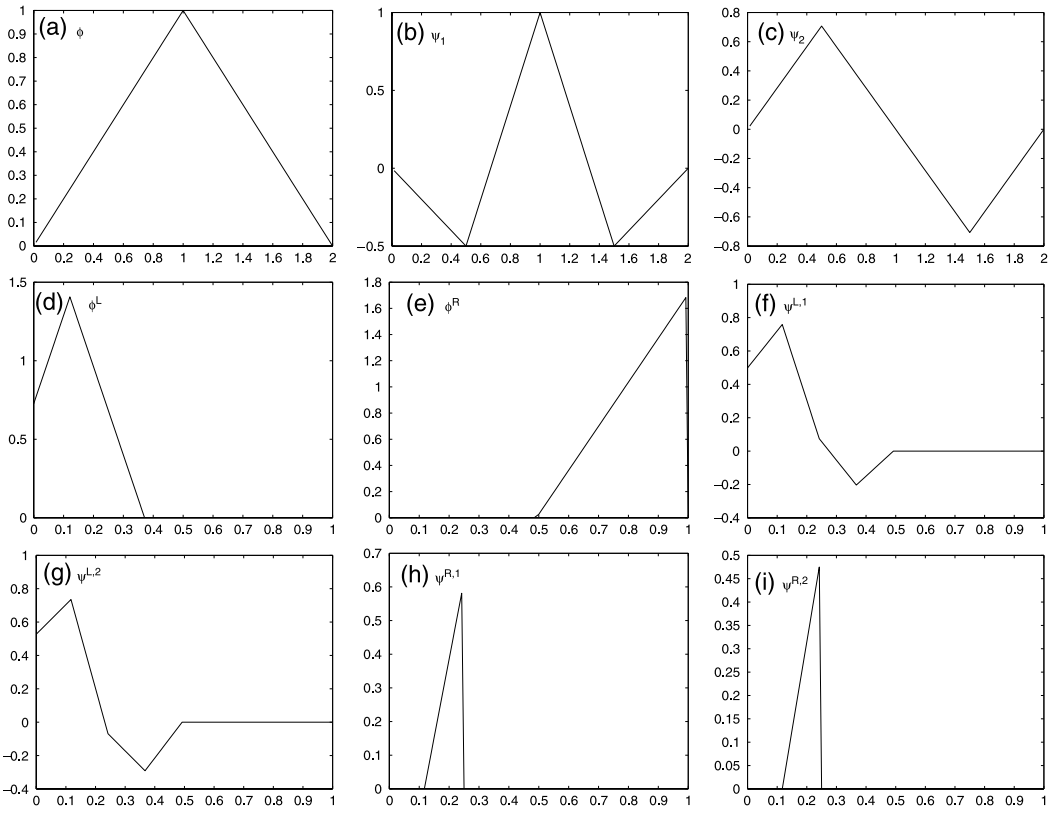

Fig. 1. Scaling function and wavelet frame on the interval corresponding to linear B-spline.

By Theorems 1 and 2, obtain the filter coefficients:

$$H = \begin{pmatrix} H^L & h^L & 0 & 0 & 0 \\ 0 & \frac{1}{2} & 1 & \frac{1}{2} & 0 \\ 0 & 0 & 0 & h^R & H^R \end{pmatrix}, \qquad G^1 = \begin{pmatrix} G^{L,1} & g^{L,1} & 0 & 0 & 0 \\ 0 & -\frac{1}{2} & 1 & -\frac{1}{2} & 0 \\ 0 & 0 & 0 & g^{R,1} & G^{R,1} \end{pmatrix},$$

$$G^2 = \begin{pmatrix} G^{L,2} & g^{L,2} & 0 & 0 & 0 \\ 0 & \frac{\sqrt{2}}{2} & 0 & -\frac{\sqrt{2}}{2} & 0 \\ 0 & 0 & 0 & g^{R,2} & G^{R,2} \end{pmatrix}.$$

By Theorem 3, there exists minimum-energy frame on the interval (see Fig. 1).

Example 2 (*Quadratic B-spline*). $P_3^2(z) = \frac{1}{8} + \frac{3}{8}z + \frac{3}{8}z^2 + \frac{1}{8}z^3$, $Q_1(z) = -\frac{\sqrt{3}}{4} + \frac{\sqrt{3}}{4}z$, $Q_2(z) = \frac{1}{8} + \frac{3}{8}z - \frac{3}{8}z^2 - \frac{1}{8}z^3$.

By Theorems 1 and 2, obtain the filter coefficients:

$$H = \begin{pmatrix} H^L & h_0^L & h_1^L & 0 & 0 & 0 & 0 & 0 \\ 0 & \frac{1}{4} & \frac{3}{4} & \frac{3}{4} & \frac{1}{4} & 0 & 0 & 0 \\ 0 & 0 & 0 & \frac{1}{4} & \frac{3}{4} & \frac{3}{4} & \frac{1}{4} & 0 \\ 0 & 0 & 0 & 0 & 0 & h_1^R & h_0^R & H^R \end{pmatrix},$$

$$G^1 = \begin{pmatrix} G^{L,1} & g_0^{L,1} & g_1^{L,1} & 0 & 0 & 0 & 0 & 0 \\ 0 & -\frac{\sqrt{3}}{2} & \frac{\sqrt{3}}{2} & 0 & 0 & 0 & 0 & 0 \\ 0 & 0 & 0 & -\frac{\sqrt{3}}{2} & \frac{\sqrt{3}}{2} & 0 & 0 & 0 \\ 0 & 0 & 0 & 0 & 0 & g_1^{R,1} & g_0^{R,1} & G^{R,1} \end{pmatrix},$$

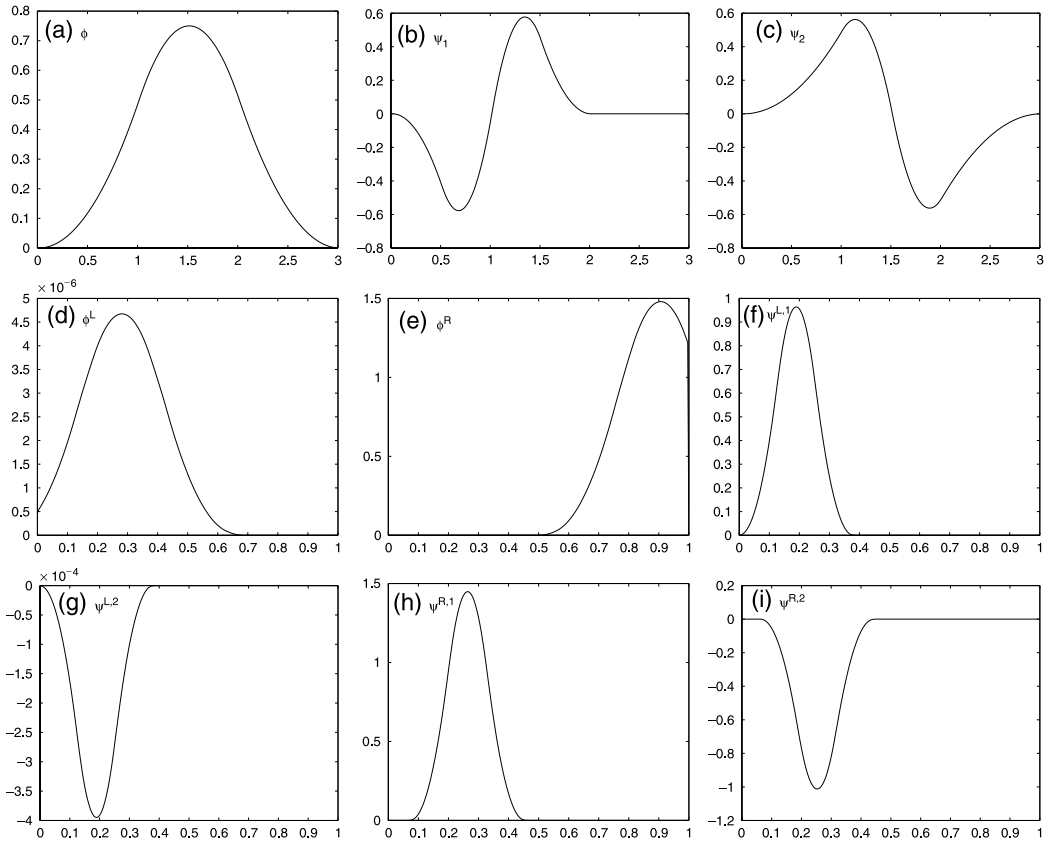

Fig. 2. Scaling function and wavelet frame on the interval corresponding to quadratic B-spline.

$$G^2 = \begin{pmatrix} G^{L,2} & g_0^{L,2} & g_1^{L,2} & 0 & 0 & 0 & 0 & 0 \\ 0 & \frac{1}{4} & \frac{3}{4} & -\frac{3}{4} & -\frac{1}{4} & 0 & 0 & 0 \\ 0 & 0 & 0 & \frac{1}{4} & \frac{3}{4} & -\frac{3}{4} & -\frac{1}{4} & 0 \\ 0 & 0 & 0 & 0 & 0 & g_1^{R,2} & g_0^{R,2} & G^{R,2} \end{pmatrix}.$$

By Theorem 3, there exists minimum-energy frame on the interval (see Fig. 2).

4.2. $d = 3$

Example 3. $P_1^3(z) = \frac{1}{3} + \frac{1}{3}z + \frac{1}{3}z^2, Q_1(z) = \frac{\sqrt{2}}{6} - \frac{\sqrt{2}}{3}z + \frac{\sqrt{2}}{6}z^2, Q_2(z) = \frac{\sqrt{6}}{6} - \frac{\sqrt{6}}{6}z^2$.

It's obvious that the scaling function ϕ and wavelet functions ψ_1, ψ_2 (see Fig. 3) are supported in [0, 1]. It's very easy to restrict the frame for $L^2(R)$ to a frame for $L[0, 1]$; starting from the collection $\{\phi_{0,k}; k \in Z\} \bigcup \{\psi_{j,k}^i; j \geq 0, k \in Z, i = 1, \ldots, M\}$, which is a frame for $L^2(R)$, we can restrict them to [0, 1] easily. Since every one of the them is supported either in [0, 1] or in $R\backslash]0, 1[$, the collection that remains after all the functions with restriction 0 has been weeded out, i.e., $\{\phi_{0,0}\} \bigcup \{\psi_{j,k}^i; j \geq 0, 0 \leq k \leq d^j, i = 1, \ldots, M\}$ is a frame for $L[0, 1]$.

Example 4. $P_2^3(z) = (\frac{1}{3} + \frac{1}{3}z + \frac{1}{3}z^2)^2, Q_1(z) = \frac{\sqrt{2}}{18} + \frac{\sqrt{2}}{9}z - \frac{\sqrt{2}}{3}z^2 + \frac{\sqrt{2}}{9}z^3 + \frac{\sqrt{2}}{18}z^4, Q_2(z) = \frac{\sqrt{6}}{18} + \frac{\sqrt{6}}{9}z - \frac{\sqrt{6}}{9}z^3 - \frac{\sqrt{6}}{18}z^4$, $Q_3(z) = \frac{2\sqrt{3}}{9} - \frac{2\sqrt{3}}{9}z$.

By Theorems 1–3, there exists minimum-energy frame on the interval (see Fig. 4).

5. Threshold-based image denoising via minimum-energy wavelet frame on the interval

In recent years, wavelets have been widely applied to various fields, especially to the image processing, such as image denoising, image compression and so on. The redundant wavelet is very suitable for image denoising. Therefore, in order

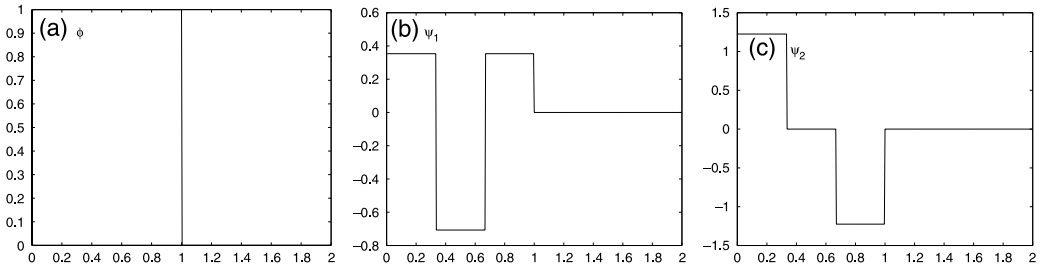

Fig. 3. Scaling function and wavelet frame on the interval corresponding to $P_1^3(z)$.

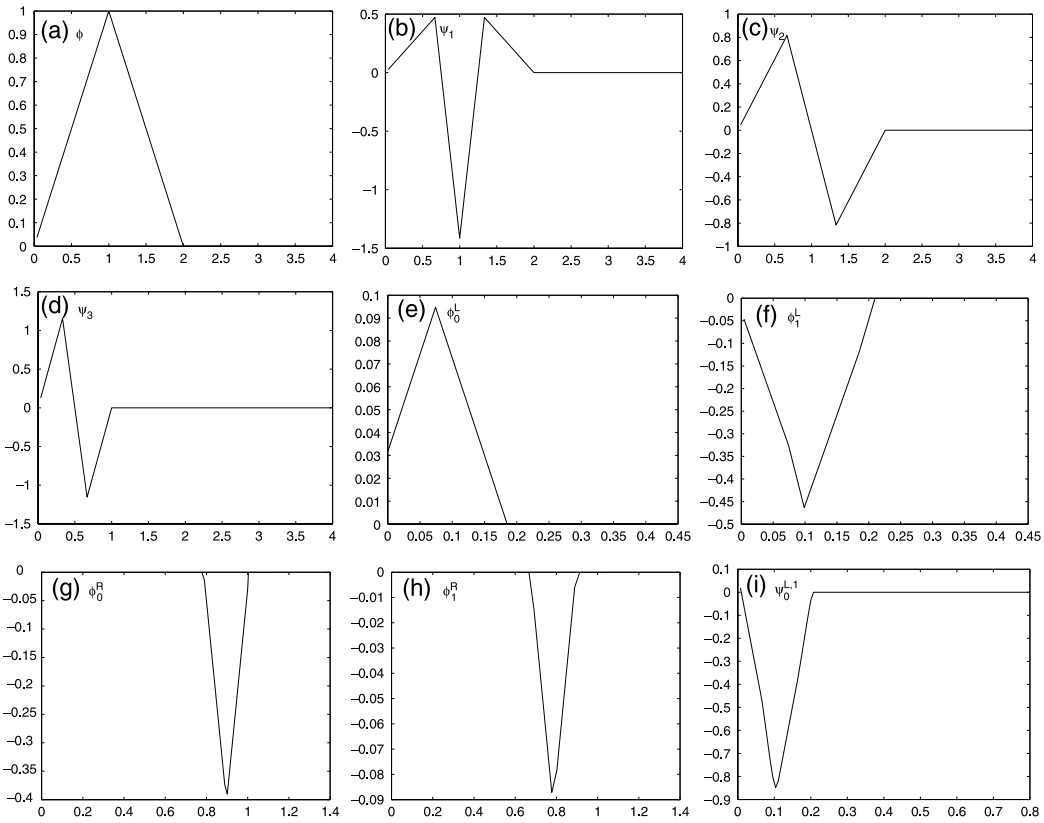

Fig. 4. Scaling function and wavelet frame on the interval corresponding to $P_2^3(z)$.

to verify the superiority of minimum-energy wavelet frame on the interval, we propose a threshold-based image denoising method via minimum-energy wavelet frame on the interval.

Suppose that an observed image y that is corrupted by additive zero-mean white Gaussian noise ε can be represented by $y = x + \varepsilon$, x represents coefficients of the "clean" image. As we're known, the redundant wavelet system coefficients of the resulting noisy signal will also be corrupted by white Gaussian noise.

We choose certain threshold for image denoising via minimum-energy frame on the interval. The process of denoising can be divided into three steps:

(1) Transform the noisy image y into wavelet coefficient w via minimum-energy frame on the interval.
(2) Apply the hard threshold t at each scale j.
(3) Perform inverse transform to obtain the denoised image.

In the step (2), we use the most well-known VisuShrink universal threshold $t = \sigma\sqrt{2\log N}$ (N is the size of the image) proposed in [17] and the robust median method divided by 0.6745 to compute the value of σ, i.e., $\sigma = MAD/0.6745$.

We test the Lena and Barbara image corrupted by additive zero-mean white Gaussian noise σ. For comparison of the denoising results, we apply such wavelets with the same support as the Daubechis orthogonal wavelet DB2 and the interval

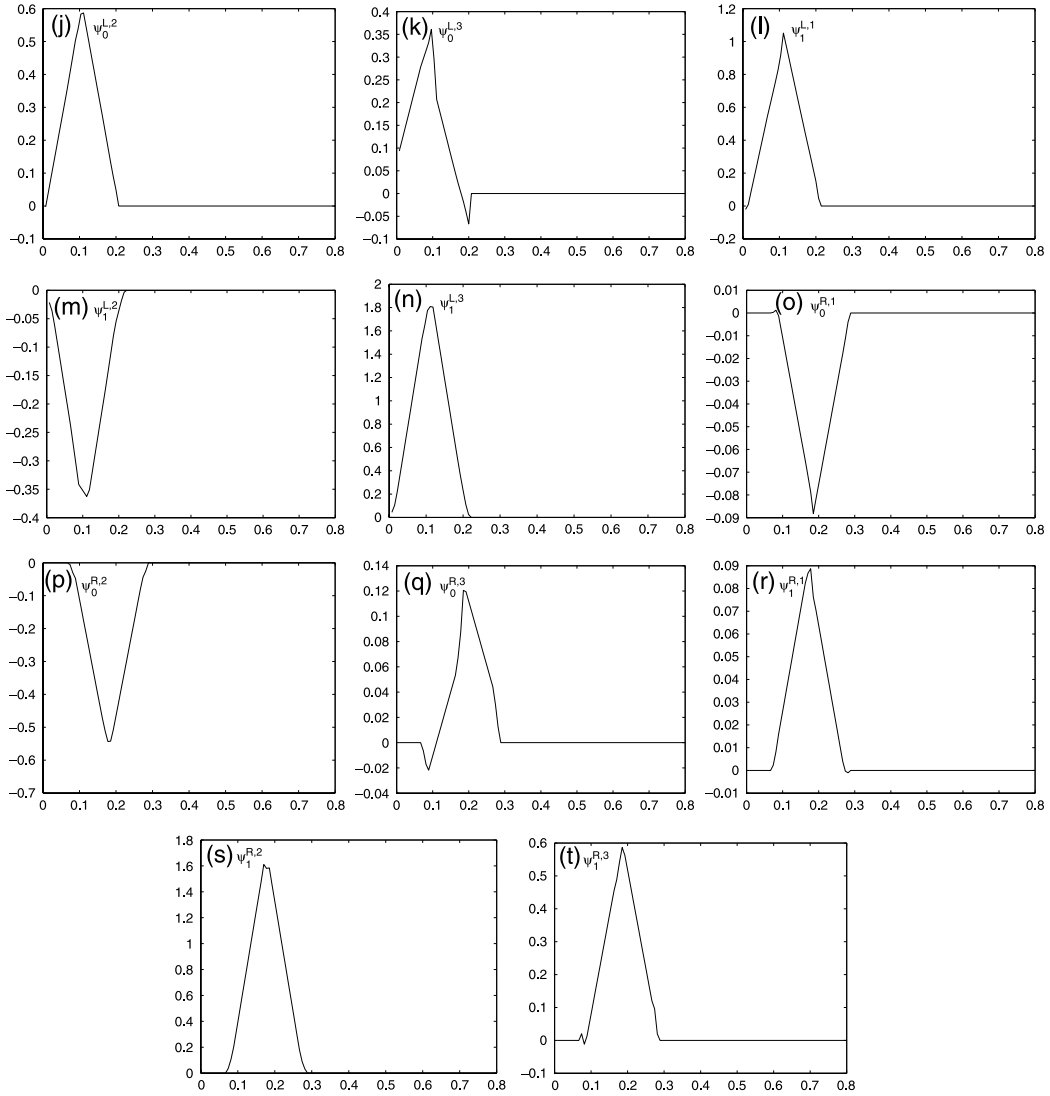

Fig. 4. (*continued*)

DB2 structured in [1] (INT-DB2), minimum-energy wavelet frame proposed in [2] (MEF, see Example 1 in [2]) and our minimum-energy wavelet frame on the interval (INT-MEF, see Example 1 in the above section), respectively. The denoising results are shown in Table 1 and Figs. 5 and 6. From the results, we see that our algorithm improves the objective quality of the denoised image in terms of signal-to-noise ratio (SNR). This shows that our minimum-energy wavelet frames on the interval is superior to orthogonal wavelets and minimum-energy wavelet frames. In fact, in the applications of image denoising, minimum-energy wavelet frame due to the symmetry/anti-symmetry and shift-invariance has better denoising performance than the orthogonal wavelets. At the same time, minimum-energy wavelet frame on the interval avoids "border effect" effectively owing to the edge wavelets maintaining the smoothness and symmetry.

6. Conclusion

The interval wavelets can solve the un-matching problem using the multi-resolution analysis for $L^2(R)$ between the signal space and the approximate space, and avoid "border effect" effectively. Wavelet frame has more stability for the reconstruction of the signal than orthogonal wavelet and biorthogonal wavelet, good time-frequency localized representations, shift-invariance, and more design freedom.

In this paper, based on the theory of the wavelet frame, we construct a class of minimum-energy wavelet frames with arbitrary factor d, obtain the necessary and sufficient conditions of the minimum-energy frames for $L^2[0, 1]$, and present the

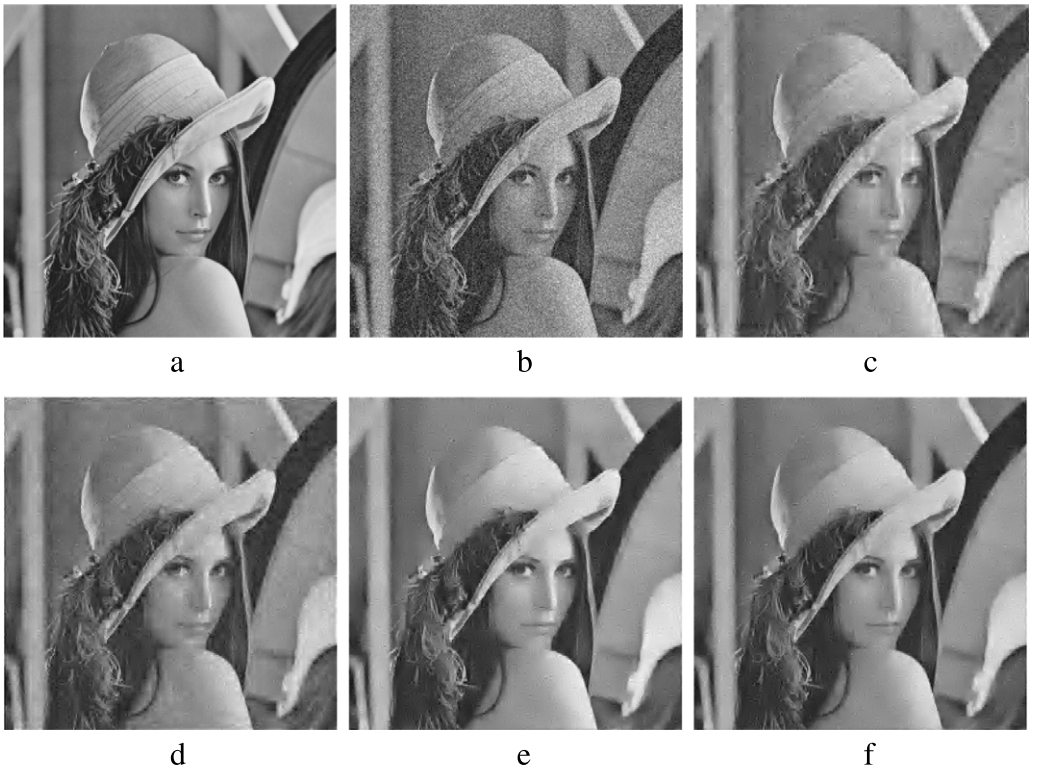

Fig. 5. Denoising results. (a) original Lena image, (b) noisy image with a white Gaussian noise with 25, (c) denoised image by DB2, (d) denoised image by INT-DB2, (e) denoised image by MEF, (f) denoised image by INT-MEF.

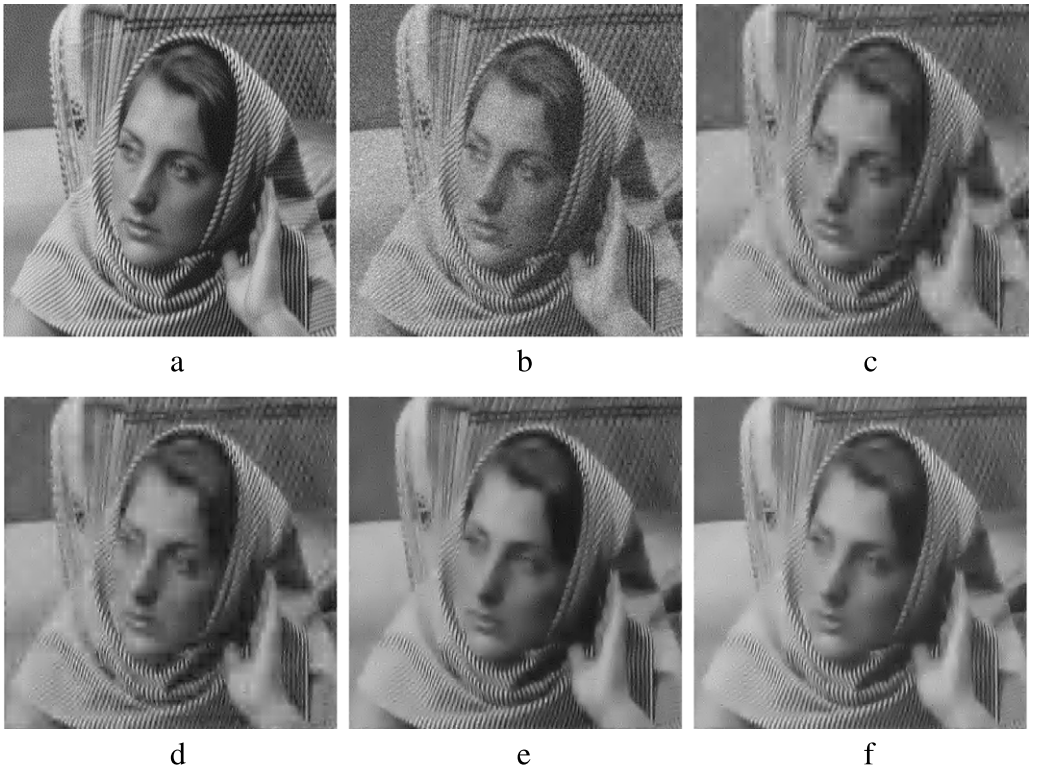

Fig. 6. Denoising results. (a) original Barbara image, (b) noisy image with a white Gaussian noise with 25, (c) denoised image by DB2, (d) denoised image by INT-DB2, (e) denoised image by MEF, (f) denoised image by INT-MEF.

Table 1
The SNR of denoised image via different wavelets.

Image	Noise variance σ	DB2	INT-DB2	MEF	INT-MEF
Lena	20	15.85	15.99	17.22	18.12
	25	12.85	12.96	14.15	14.79
	30	9.71	10.01	10.98	11.65
Barbara	20	14.73	14.76	15.29	15.79
	25	12.17	12.31	13.11	13.95
	30	9.53	9.73	10.40	11.13

decomposition and reconstruction algorithms. The experimental results in the application of image denoising show that our minimum-energy wavelet frames on the interval is superior to orthogonal wavelets and minimum-energy wavelet frames.

References

[1] A. Cohen, I. Daubechies, P. Vial, Wavelets on the interval and fast wavelet transforms, Appl. Comput. Harmon. Anal. 1 (1) (1993) 54–81.
[2] C.K. Chui, W. He, Compactly supported tight frames associated with refinable functions, Appl. Comput. Harmon. Anal. 8 (3) (2000) 293–319.
[3] Yongdong Huang, Zhengxing Cheng, Minimum-energy frames associated with refinable function of arbitrary integer dilation factor, Chaos Solitons Fractals 32 (2007) 503–515.
[4] I.W. Selesnick, Smooth wavelet tight frames with zero moments, Appl. Comput. Harmon. Anal. 10 (2) (2001) 163–181.
[5] A. Farras Abdelnour, I.W. Selesnick, Symmetric nearly shift-invariant tight frame wavelets, IEEE Trans. Signal Process. 53 (1) (2005) 231–238.
[6] I.W. Selesnick, Symmetric wavelet tight frames with two generators, Appl. Comput. Harmon. Anal. 17 (2) (2004) 211–225.
[7] C.K. Chui, W. He, J. Stöckler, Compactly supported tight and sibling frames with maximum vanishing moments, Appl. Comput. Harmon. Anal. 13 (3) (2003) 177–283.
[8] Alexander Petukhov, Explicit construction of framelets, Appl. Comput. Harmon. Anal. 11 (2001) 313–327.
[9] I. Daubechies, B. Han, A. Ron, Z. Shen, Framelets: MRA-based constructions of wavelet frames, Appl. Comput. Harmon. Anal. 14 (1) (2003) 1–46.
[10] Q.T. Jiang, Parameterizations of masks for tight affine frames with two symmetric/antisymmetric generators, Adv. Comput. Math. 18 (2003) 247–268.
[11] A. Petukhov, Symmetric framelets, Constr. Approx. 19 (2) (2003) 309–328.
[12] I.W. Selesnick, L. S'endur, Smooth wavelet frames with application to denoising, in: IEEE Proc. Int. Conf. Acoust., Speech and Signal Processing, Istanbul, Turkey, 2000,1: pp. 129–132.
[13] K. Grochenig, A. Pon, Tight compactly supported wavelet frames of arbitarily high smoothness, Proc. Amer. Math. Soc. 126 (4) (1998) 1101–1110.
[14] H. Bölcskei, F. Hlawatsch, Oversampled cosine modulated filter banks with perfect reconstruction, IEEE Trans. Circuits Syst. II 45 (1998) 1057–1071.
[15] J.J. Benedetto, O.M. Treiber, Wavelet frame: multiresolution analysis and extension principle, in: L. Ebnath (Ed.), Wavelet Transform and Time-Frequency Signal Analysis, Birkhauser, Boston, 2000.
[16] Xieping Gao, Siwang Zhou, A study of orthogonal, balanced and symmetric multi-wavelets on the interval, Science in China Ser.F Information Sciences 48 (6) (2005) 761–781.
[17] D.L. Donoho, I.M. Johnstone, Ideal spatial adaptation by wavelet shrinkage, Biometrika 81 (3) (1994) 425–455.